



**HAL**  
open science

## The AF-1-deficient estrogen receptor ER $\alpha$ 46 isoform is frequently expressed in human breast tumors

Elodie Chantalat, Frédéric Boudou, Henrik Laurell, Gaëlle Palierne, René Houtman, Diana Melchers, Philippe Rochaix, Thomas Filleron, Alexandre Stella, Odile Burlet-Schiltz, et al.

### ► To cite this version:

Elodie Chantalat, Frédéric Boudou, Henrik Laurell, Gaëlle Palierne, René Houtman, et al.. The AF-1-deficient estrogen receptor ER $\alpha$ 46 isoform is frequently expressed in human breast tumors. *Breast Cancer Research*, 2016, 18 (1), pp.123. 10.1186/s13058-016-0780-7. inserm-01412032

**HAL Id: inserm-01412032**

**<https://inserm.hal.science/inserm-01412032>**

Submitted on 7 Dec 2016

**HAL** is a multi-disciplinary open access archive for the deposit and dissemination of scientific research documents, whether they are published or not. The documents may come from teaching and research institutions in France or abroad, or from public or private research centers.


L'archive ouverte pluridisciplinaire **HAL**, est destinée au dépôt et à la diffusion de documents scientifiques de niveau recherche, publiés ou non, émanant des établissements d'enseignement et de recherche français ou étrangers, des laboratoires publics ou privés.

RESEARCH ARTICLE

Open Access



# The AF-1-deficient estrogen receptor ERα46 isoform is frequently expressed in human breast tumors

Elodie Chantalat<sup>1,2</sup>, Frédéric Boudou<sup>1</sup>, Henrik Laurell<sup>1</sup>, Gaëlle Palierne<sup>3</sup>, René Houtman<sup>4</sup>, Diana Melchers<sup>4</sup>, Philippe Rochaix<sup>2</sup>, Thomas Filleron<sup>2</sup>, Alexandre Stella<sup>5</sup>, Odile Burlet-Schiltz<sup>5</sup>, Anne Brouchet<sup>2</sup>, Gilles Flouriot<sup>6</sup>, Raphaël Métivier<sup>3</sup>, Jean-François Arnal<sup>1</sup>, Coralie Fontaine<sup>1</sup> and Françoise Lenfant<sup>1\*</sup> 

## Abstract

**Background:** To date, all studies conducted on breast cancer diagnosis have focused on the expression of the full-length 66-kDa estrogen receptor alpha (ERα66). However, much less attention has been paid to a shorter 46-kDa isoform (ERα46), devoid of the N-terminal region containing the transactivation function AF-1. Here, we investigated the expression levels of ERα46 in breast tumors in relation to tumor grade and size, and examined the mechanism of its generation and its specificities of coregulatory binding and its functional activities.

**Methods:** Using approaches combining immunohistochemistry, Western blotting, and proteomics, antibodies allowing ERα46 detection were identified and the expression levels of ERα46 were quantified in 116 ERα-positive human breast tumors. ERα46 expression upon cellular stress was studied, and coregulator bindings, transcriptional, and proliferative response were determined to both ERα isoforms.

**Results:** ERα46 was expressed in over 70% of breast tumors at variable levels which sometimes were more abundant than ERα66, especially in differentiated, lower-grade, and smaller-sized tumors. We also found that ERα46 can be generated via internal ribosome entry site-mediated translation in the context of endoplasmic reticulum stress. The binding affinities of both unliganded and fully-activated receptors towards co-regulator peptides revealed that the respective potencies of ERα46 and ERα66 differ significantly, contributing to the differential transcriptional activity of target genes to 17β estradiol (E2). Finally, increasing amounts of ERα46 decrease the proliferation rate of MCF7 tumor cells in response to E2.

**Conclusions:** We found that, besides the full-length ERα66, the overlooked ERα46 isoform is also expressed in a majority of breast tumors. This finding highlights the importance of the choice of antibodies used for the diagnosis of breast cancer, which are able or not to detect the ERα46 isoform. In addition, since the function of both ERα isoforms differs, this work underlines the need to develop new technologies in order to discriminate ERα66 and ERα46 expression in breast cancer diagnosis which could have potential clinical relevance.

**Keywords:** Breast cancer, Estrogen receptor ERα, Isoforms, Diagnosis, Internal ribosomal entry site, Activation function

\* Correspondence: francoise.lenfant@inserm.fr

<sup>1</sup>INSERM U1048, Institut des Maladies Métaboliques et Cardiovasculaires, Université de Toulouse, BP 84225, 31 432 Toulouse cedex 04, France  
Full list of author information is available at the end of the article

## Background

Breast cancer is a major public health concern because its incidence continues to rise. It is the second most common cancer overall and by far the most frequent cancer among women [1]. The etiology of breast cancer is multifactorial, and although the mechanisms of carcinogenesis remain poorly defined the role of hormones is recognized as a major risk factor in breast cancer development, in particular  $17\beta$  estradiol (E2) and its derivatives.

Estrogen receptor (ER) $\alpha$  is one of two ERs and is involved in several key aspects of breast cancer diagnosis [2]. Firstly, ER $\alpha$  protein immunoreactivity in the nucleus of mammary epithelial cells is systematically evaluated and quantified during anatomopathological diagnosis, with 70% of breast cancers initially described as ER $\alpha$ -positive [2]. Secondly, ER $\alpha$  expression in breast cancers correlates with improved survival rates and reduced risk of recurrence and metastases [3–5]. Finally, the blockade of ER $\alpha$  activity represents a major targeted therapy for ER $\alpha$ -positive breast cancer, with tamoxifen and aromatase inhibitors having already benefitted millions of women [6]. Despite the success of these treatments, 30 to 40% of patients develop resistance [7]. This highlights the need for further in-depth characterization of ER $\alpha$ -positive tumors and a full understanding of the mechanisms underlying the disease in order to propose new therapeutic approaches.

In addition to the “classic” full-length 66-kDa ER $\alpha$  (ER $\alpha$ 66) which harbors the two activation functions, AF-1 and AF-2, two other isoforms of 46 kDa (ER $\alpha$ 46) and 36 kDa (ER $\alpha$ 36) have been characterized. ER $\alpha$ 36 differs from ER $\alpha$ 66 by lacking both transcriptional activation domains (AF-1 and AF-2) and encoding a unique 29 amino acid sequence [8]. In contrast, ER $\alpha$ 46 only lacks the first 173 N-terminal amino acids which harbors AF-1 and is thus completely identical to the amino acids 174 to 595 of ER $\alpha$ 66 (Fig. 1a). ER $\alpha$ 46 has been reported to be expressed in various cell types such as human osteoblasts [9], macrophages [10], and vascular endothelial cells [11], but also in cancer cells such as colorectal tumor tissues [12] and tamoxifen-resistant breast cancer cell lines [13]. Mechanisms regulating both the expression of ER $\alpha$ 46 and its functions remain essentially unknown. It can be generated by either alternative splicing [14], proteolysis [15], or an alternative initiation of translation via an internal ribosome entry site (IRES) [16]. This latter mechanism generates two different proteins from a single RNA. A few studies have suggested that ER $\alpha$ 46 plays an inhibitory role in the growth of cancer cell lines, suggesting that ER $\alpha$ 46 could affect tumor progression. The overexpression of ER $\alpha$ 46 in proliferating MCF7 cells provoked cell cycle arrest in G0/G1 phase and inhibited ER $\alpha$ 66-mediated estrogenic induction of the AF-1-sensitive reporters *c-fos* and cyclin D1, as well as estrogen-responsive element (ERE)-driven reporters [14, 17]. It was also shown that ER $\alpha$ 46 inhibits growth and induces apoptosis in human

HT-29 colon adenocarcinoma cells [12]. This inhibition likely occurs through competition between ER $\alpha$ 66 and ER $\alpha$ 46 homodimers and heterodimers for binding to the ERE [17]. The role of the AF-1-deficient ER $\alpha$ 46 isoform has also been questioned in vivo using mice deficient in the ER $\alpha$  A/B domain (named *ER $\alpha$ AF-1<sup>0</sup>*), which express only a short 49-kDa isoform that is functionally similar to ER $\alpha$ 46. These *ER $\alpha$ AF-1<sup>0</sup>* mice revealed a complete infertility phenotype [18] that was associated with an altered proliferative effect of E2 on the uterine epithelium and a loss of its transcriptional response in this tissue [19].

Thus, the roles and functions of this ER $\alpha$ 46 isoform appear to be different from those of full-length ER $\alpha$ 66. The expression level of this truncated isoform in human breast tumors remains unknown, even though the expression of a 47-kDa isoform of ER $\alpha$  in human breast cancers was reported more than two decades ago [20]. Currently, several antibodies are used for immunohistochemical detection of ER $\alpha$  in human breast tumor diagnosis but most of them have not yet been thoroughly characterized in terms of ER $\alpha$ 46 recognition.

In this study, we first characterized the various antibodies commonly employed in immunohistochemical diagnosis for their ability to detect ER $\alpha$ 46. We then analyzed the relative expression of the ER $\alpha$  isoforms in a panel of 116 ER $\alpha$ -positive breast tumors. We also examined the mechanism of ER $\alpha$ 46 generation and its specificities in term of coregulator binding and of functional activities.

## Methods

### Cell culture

MDA-MB231 and MDA-MB231 cells stably expressing ER $\alpha$ 66 (MDA-ER $\alpha$ 66; [21]) or ER $\alpha$ 46 (MDA-ER $\alpha$ 46; [22]) or transiently transfected with pSG5Flag-ER $\alpha$ 36 (kindly provided by M. Le Romancer) were maintained in Dulbecco's modified Eagle's medium (DMEM; Sigma) supplemented with 5% fetal calf serum (FCS; Biowest) and antibiotics (Sigma) at 37 °C under 5% CO<sub>2</sub>. Media used to maintain cells expressing either ER isoforms also included hygromycin (Calbiochem; 0.8 mg/ml). We also transiently transfected MDA cells with either the pcDNA3.1 plasmid, encoding the cDNA of ER $\alpha$ 46, or a mutated version, ER $\alpha$ 46kDa<sup>0</sup>, using the *TransIT*<sup>®</sup>-BrCa Transfection Reagent (Euromedex, France). This mutated plasmid was obtained by subcloning a fragment from ER $\alpha$ 66 that contains an AUG/UCG mutation at codon 174 and an AUG/AUA mutation at codon 176 [16]. Stably transfected MCF7 sub-clones MCF7-B0 (control) and MCF7-B1 and MCF7-B2 overexpressing ER $\alpha$ 46 were obtained by transfecting MCF7 cells with pcDNA6/TR plasmid and pcDNA4/TO expression vector containing or not the ER $\alpha$ 46 cDNA sequence (T-Rex system, Invitrogen) with jetPEI reagent (Polyplus transfection). The clones were selected with 5  $\mu$ g/ml blasticidin and 100  $\mu$ g/ml zeocin (Invitrogen). Individual clones were

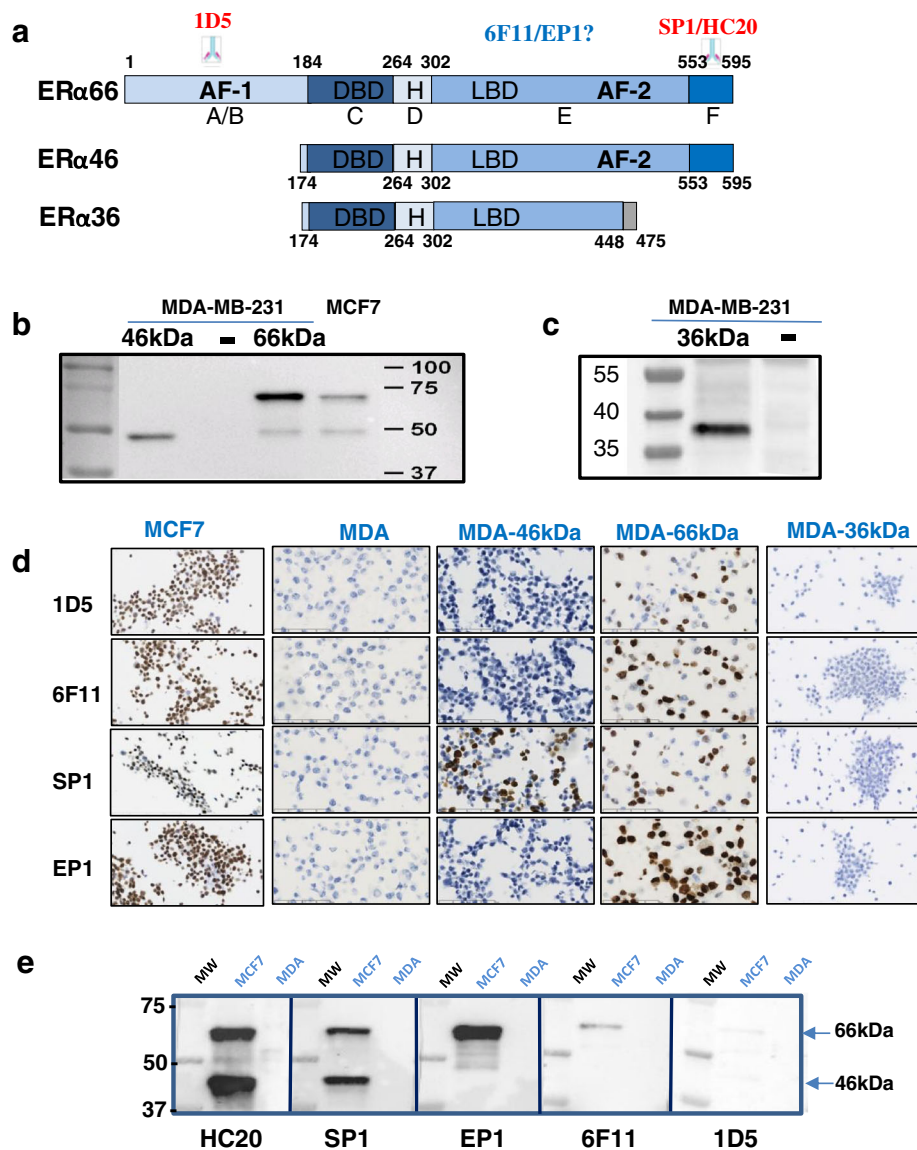


**Fig. 1** Recognition of estrogen receptor alpha (*Era*) isoforms by antibodies used for human breast cancer diagnosis. **a** Schematic representation of the ERα66, ERα46, and ERα36 isoforms. The location of the known epitopes used for the generation of antibodies is indicated. **b** Representative Western blot analyses with the SP1 antibody on extracts from MDA-MB-231 cells transfected with plasmids encoding either ERα46 (MDA-46 kDa) or ERα66 (MDA-66 kDa) and from MCF7 cells which express both isoforms, or **c** with the Anti-Flag antibody on extracts from MDA-MB-231 cells transfected with plasmids encoding the ERα36 isoform. **d** The different antibodies used in breast cancer diagnosis (1D5, 6 F11, SP1, and EP1) were tested for their ability to recognize either ERα66, ERα46, or both isoforms in immunocytochemistry experiments performed in MCF7, MDA-ERα46, and MDA-ERα66 or MDA-ERα36 cells. **e** Representative picture of Western blot experiments evaluating the expression of both ERα isoforms in MCF-7 cells, as determined by the different antibodies indicated. Protein extracts prepared from MDA cells were used as an ERα-negative control. AF activation function, DBD DNA-binding domain, LBD ligand-binding domain

isolated and grown in a medium containing selective antibiotics to maintain selection pressure. Expression of the proteins of interest was induced by a 48-h treatment of MCF7 sub-clones with 1 µg/ml tetracyclin.

#### Immunohistochemistry

Cells were formalin-fixed and paraffin-embedded using the Shandon™ CytoBlock™ Cell Block Preparation System,

according to the manufacturer's protocol. Immunohistochemistry was performed with a Dako Autostainer Link 48 on 3-µm sections. Antigen retrieval was performed using a Dako PT Link pressure cooker in pH 6.0 citrate buffer. An EnVision™ system was used for antibody detection. The anti-ERα antibodies (SP1 (Abcam), HC20 (SantaCruz), 6 F11 (Novocastra), 1D5 and EP1 (Dako)) were used.

### Human breast cancer sample collection

The retrospective study used tumors samples from patients diagnosed with invasive breast carcinoma, established as being ER $\alpha$ -positive on a previously performed biopsy (see Additional file 1 (Figure S1) for clinical parameters of the patients used). The diagnosis was performed with the 6 F11 or 1D5 antibodies between 2011 and 2014. Tumors were frozen in 1.5-ml cryotubes using the Snap-FrostII™ fast freezing system (Excilone, France) and stored at  $-80^{\circ}\text{C}$ . Patients with an ipsilateral recurrence of breast cancer who had received neoadjuvant chemotherapy or chemotherapy treatment for another disease or who received thoracic radiation therapy (recurrence or another pathology) were excluded. All tumors were classified by the anatomopathologist (human epidermal growth factor receptor-2 (HER2) status, tumor size, ER $\alpha$  overexpression, lymph node involvement, histological type) and were graded according to Elstone and Ellis' guidelines [23]. The analysis was performed on a series of 116 ER $\alpha$ -positive invasive ductal or lobular breast carcinomas (22 grade I, 60 grade II, and 34 grade III).

### Western blots on tumor samples

Samples of each tumor were lysed in cold lysis buffer (150 mM NaCl, 50 mM Tris-HCl pH 7.5, 0.1% SDS, 1 mM ethylenediaminetetraacetic acid (EDTA), 5 mM NaF, 1 mM orthovanadate, 0.5 mM 1,4-dithiothreitol (DTT), and protease inhibitors) using a Precellys Homogeniser (Bertin Technologies, France). Proteins were separated on a 10% SDS-PAGE gel and transferred to a nitrocellulose membrane. After blocking, membranes were incubated overnight with the primary antibody (anti-ER $\alpha$  (SP1) or anti-GAPDH (6C5); Santa Cruz). Subsequently, blots were incubated with a horseradish peroxidase (HRP)-conjugated secondary antibody (anti-rabbit; Cell Signaling) and visualized by enhanced chemiluminescence (ECL) detection according to the manufacturer's instructions (Amersham Biosciences, CT) using a ChemiDoc™ Imaging System (Bio-Rad). Bands corresponding to ER $\alpha$ 46 and ER $\alpha$ 66 were quantified using ImageJ densitometry, and the ratio of the band intensities was calculated.

### Endoplasmic reticulum stress

MDA-66 kDa or MCF7 cells were seeded in six-well plates. At 80% confluence, the cells were subjected to 6 h of stress with DTT (Euromedex) or thapsigargin (Sigma) as indicated, then rinsed in phosphate-buffered saline (PBS), lysed in SDS buffer (5% SDS, 10% glycerol, 80 mM Tris pH6.8), and sonicated. Western blot analyses were then performed on 4–20% denaturing polyacrylamide “stain-free” gels (BioRad).

### Immunoprecipitation and proteomic analysis

ER $\alpha$ -enriched protein fractions from tumor protein extracts were obtained through immunoprecipitation using the anti-human ER $\alpha$  primary HC20 antibody. Following their

purification using Protein G sepharose beads, a first Western blot was performed to check the efficiency of the immunoprecipitation. In parallel, the immunoprecipitate was diluted with Laemmli buffer, then separated by SDS-PAGE using a short and low-voltage electrophoretic migration. After Instant Blue staining, the bands corresponding to ER $\alpha$ 46 and ER $\alpha$ 66 were respectively excised from the gel. Proteins were in-gel digested by trypsin, and resulting peptides were extracted from the gel and analyzed by nano-liquid chromatography coupled to tandem mass spectrometry (LC-MS/MS) using an ultimate 3000 system (Dionex, Amsterdam, Netherlands) coupled to an LTQ-Orbitrap Velos mass spectrometer (Thermo Scientific, Bremen, Germany).

The LTQ-Orbitrap Velos was operated in data-dependent acquisition mode with the Xcalibur software. Survey scan MS spectra were acquired in the Orbitrap in the 300–2000  $m/z$  range with the resolution set to a value of 60,000. The twenty most intense ions per survey scan were selected for collision-induced dissociation fragmentation, and the resulting fragments were analyzed in the linear ion trap (LTQ, parallel mode, target value  $1e4$ ). Database searches from the MS/MS data were performed using the Mascot Daemon software (version 2.3.2, Matrix Science, London, UK). The following parameters were set for creation of the peak lists: parent ions in the mass range 400–4500, no grouping of MS/MS scans, and threshold at 1000. Data were searched against SwissProt 20130407. Mascot results were parsed with the in-house developed software MFPaQ version 4.0 (Mascot File Parsing and Quantification) (<http://mfpaq.sourceforge.net/>) and protein hits were automatically validated with a false discovery rate (FDR) of 1% on proteins and 5% on peptides (minimum peptide length of six amino acids).

### Plasmids, lentiviral production, and luciferase assay

cDNA coding for the A/B (amino acids 2–173) domain of the human *ESR1* gene encoding ER $\alpha$  was amplified by polymerase chain reaction (PCR) and cloned into the *SpeI* and *NcoI* sites of the pTRIP CRF1AL2 bi-cistronic vector that encodes both the Renilla luciferase (LucR) and Firefly luciferase (LucF2CP) genes separated by this putative IRES-ER $\alpha$  sequence [24]. The final construct was verified by sequencing. In such a transgene, LucR expression is cap-dependent whereas LucF expression is IRES-dependent; thus, the level of IRES activity can be deduced from the LucF/LucR ratio. The production of lentiviral particles was performed in HEK293 cells. Transduced MDA-MB 231 cells (MDA-A/B) were subjected to ER stress as indicated. To test whether the stress-induced increase in LucF activity was not due to the generation of mono-cistronic LucF transcripts via an internal promoter or cryptic splicing, MDA-Lenti-AB (1/10) cells were exposed to two siRNAs-lucR and treated with 5 mM DTT or 100 nM thapsigargin. As control, cells were treated with scrambled siRNA. After a PBS wash, cells were



frozen at  $-80^{\circ}\text{C}$ . Luciferase measurements were performed with a LB960 luminometer (Berthold) using the dual reporter assay kit (E1960; Promega) according to the manufacturer's recommendations.

### RT-qPCR

MDA-MB231, MDA-ER $\alpha$ 46, and MDA-ER $\alpha$ 66 cells were plated in 9-cm diameter dishes in DMEM/0.5% charcoal-stripped FCS (csFCS) containing appropriate antibiotics in order to reach confluency 3 days later. Cells were then treated with  $10^{-8}$  M E2 final for 4 h or with a similar volume of ethanol (vehicle). Total RNAs were then purified using the Trizol™ reagent (Life Technologies, Inc.) according to the manufacturer's instructions. RNA (2  $\mu\text{g}$ ) was used as a template for reverse transcription (RT) by the M-MLV reverse transcriptase (Invitrogen) and Pd(N)6 random hexamers (Amersham Pharmacia Biosciences). Quantitative PCR used on 2  $\mu\text{l}$  of 1/10th diluted RT reactions and 1  $\mu\text{M}$  of specific oligonucleotides and were performed on BioRad CFX96 machines using BioRadIQ SYBR Green supermix with 50 rounds of amplification followed by determination of melting curves. Primers for RT-PCR were designed under the QuantPrime design tool (<http://www.quantprime.de> [25]). Independent triplicate experiments were conducted twice, and all values were normalized to *Rplp0* mRNA. Significant variations were evaluated using the GraphPadPrism™ software.

### Coregulator-peptide interaction profiling

Ligand-mediated modulation of the interactions between the ER $\alpha$ 46 and ER $\alpha$ 66 proteins and their coregulators was characterized by a MARCoNI (Microarray Assay for Real-time Coregulator-Nuclear receptor Interaction; PamGene International BV, the Netherlands). This method has been described previously [26, 27]. Briefly, each array was incubated with a reaction mixture of crude lysates from MDA-MB-231 cells stably expressing each isoform of ER $\alpha$ 46 or ER $\alpha$ 66 on buffer F (PV4547; all Invitrogen) and vehicle (2% DMSO in water) with or without the receptor ligands at the indicated concentrations. ER $\alpha$ 66 was quantified by enzyme-linked immunosorbent assay (ELISA; Active Motif, USA) and ER $\alpha$ 46 was normalized to ER $\alpha$ 66 by Western blot analyses. SP1 antibody which specifically recognized both isoforms was used to detect the ER $\alpha$  bound on the PamChip microarray. For both ER $\alpha$ 46 and ER $\alpha$ 66 receptors, a dose-response curve was performed from  $10^{-12}$  to  $10^{-7}$  M E2 to directly compare their response to E2. For measurements of antagonist effects with 4-hydroxytamoxifen and Fulvestrant, 6.3 nM ( $10^{-8.2}$ M) E2 was applied since both receptors were fully active at that concentration. Incubation was performed at  $20^{\circ}\text{C}$  in a PamStation96 (PamGene International). Receptor binding to each peptide on the array was detected by SP1 antibody. The secondary anti-

rabbit antibody conjugated to fluorescein and the goat anti-mouse antibody conjugated to fluorescein were used and given a fluorescent signal, which was further quantified by analysis of .tiff images using BioNavigator software (PamGene International).

### Statistical analyses

Comparisons between groups were performed using the Mann-Whitney rank sum test for continuous variables. Correlations between continuous variables were evaluated using the Spearman's rank correlation test. All *P* values are two-sided. For all statistical tests, differences were considered significant at the 5% level. Statistical analyses were performed using the STATA 13.0 software (STATA Corp, College Station, TX) or GraphPad Prism v.5.

## Results

### Characterization of the anti-ER $\alpha$ antibodies commonly used for breast tumor diagnosis

Apart from lacking the A/B domain and thus the AF-1 transactivation function, the ER $\alpha$ 46 isoform is completely identical to the ER $\alpha$ 66 isoform (Fig. 1a). Therefore, to characterize the expression of ER $\alpha$ 46 in breast tumors, an antibody must be used that is directed against the C-terminal domain. This excludes 1D5, one of the first monoclonal antibodies to be available against ER $\alpha$  for tumor diagnosis [28], targeting an epitope in the A/B domain (Fig. 1a). Later on, the respective murine and rabbit monoclonal antibodies 6 F11 and SP1, with improved specificities compared to the 1D5 clone, became extensively used for diagnosis [29, 30]. More recently, the monoclonal rabbit antibody EP1 was commercialized. However, whereas the SP1 epitope is known to be in the C-terminal domain, the abilities of the 6 F11 and EP1 antibodies to recognize ER $\alpha$ 46 have not, to our knowledge, been reported.

To test this, we used control ER $\alpha$ -negative MDA-MB-231 cells and MDA cells engineered to stably express either the ER $\alpha$ 46 or ER $\alpha$ 66 isoform or to transiently express the Flag-tagged ER $\alpha$ 36 protein, alongside MCF7 cells co-expressing both proteins (Fig. 1b and c, and Additional file 1: Figure S2).

Interestingly, a small amount of ER $\alpha$ 46 expression was found in MDA 66-kDa cells, presumably due to an alternative initiation of translation at Met 174 and/or Met 176 as previously suggested [16]. Immunocytochemistry performed on these five cell lines demonstrated that, among the four tested antibodies (1D5, 6 F11, SP1, and EP1), only SP1 was able to specifically detect the ER $\alpha$ 46 isoform in the MDA 46-kDa cells (Fig. 1e). Of note, none of these antibodies was able to recognize the ER $\alpha$ 36 isoform by immunocytochemistry.

The immunoreactivity of the different antibodies was also tested by immunoblotting with the HC-20 antibody, which is frequently used in Western blot analyses, but not for diagnosis since it is a polyclonal rabbit antibody (Fig. 1e). Whereas EP1 and 6 F11 only detected ER $\alpha$ 66, the HC-20 and SP1

antibodies recognized both ER $\alpha$ 46 and ER $\alpha$ 66, which is well in line with the immunocytochemistry results. We also noticed that the 1D5 antibody had a quasi-undetectable reactivity when used in this procedure. Altogether, these data demonstrate that from the set of antibodies commonly used for breast cancer diagnosis, the SP1 antibody is the only one able to recognize the ER $\alpha$ 46a isoform by immunohistochemistry.

#### Quantification of ER $\alpha$ 46 in human breast carcinomas

Using SP1 antibody, we next performed Western blotting of 116 ER $\alpha$ -positive breast tumor samples (initially characterized with the 6 F11 or 1D5 antibodies) to compare the relative abundance of ER $\alpha$ 46 and ER $\alpha$ 66. Patients included in this study had not have received any neoadjuvant therapy. Most of the breast tumors (70%) expressed both isoforms, though at varying levels (Fig. 2a and b). The ER $\alpha$ 46/ER $\alpha$ 66 ratio varied from 0 to 3.48, with a mean average of 0.37 and a median of 0.16. Furthermore, even though the vast majority of tumors expressed lower levels of ER $\alpha$ 46 than ER $\alpha$ 66, 10% of the tumors tested expressed predominantly the shorter isoform (Fig. 2c).

We next analyzed the relationship between clinical parameters (grade and size of tumor) and ER $\alpha$ 46 expression. We found that high-grade tumors correlated with lower ER $\alpha$ 46 expression since 91% of grade I tumors expressed ER $\alpha$ 46, whereas this figure was 75 and 62% for grades II and III, respectively (Fig. 2d). Moreover, the ER $\alpha$ 46/ER $\alpha$ 66 ratio of the relative expression of these isoforms was also significantly higher in low-grade tumors compared to tumors of grades II and III which are highly dedifferentiated ( $P = 0.0024$  and  $P = 0.0059$ , respectively; see Fig. 2e). The abundance of ER $\alpha$ 46 was also inversely correlated with tumor size (Fig. 2f). Finally, we classified our samples using a size parameter usually used by the American Joint Committee on Cancer (AJCC) to characterize tumor evolution, which is set at a 2-cm cut-off. Using this classification, we found that ER $\alpha$ 46 expression was higher in small-sized tumors compared to tumors greater than 2 cm in diameter ( $P = 0.0039$ ; Fig. 2g). Interestingly, even though there was a few HER2-positive tumors among our samples, a significant correlation was found between HER2 expression and expression of ER $\alpha$ 46, indicating that HER2-positive tumors have low abundance of ER $\alpha$ 46 (Additional file 1: Figure S3). All other parameters, including necrosis, were not significant.

A few studies have shown that 8% of tumors diagnosed as ER $\alpha$ -negative using the 1D5 antibody were actually positive for ER $\alpha$  when tested with next-generation antibodies such as SP1 [29–31]. The authors did not take into account the presence of ER $\alpha$ 46, which cannot be detected by the 1D5 antibody. We therefore explored the possibility that these tumors may not express ER $\alpha$ 66 but only ER $\alpha$ 46 by evaluating the expression of the

ER $\alpha$ 46 isoform in a series of 19 tumors identified as ER $\alpha$ -negative using the 6 F11 antibody. However, none of these samples were found to express the short ER $\alpha$ 46 isoform. A representative sample is shown in Fig. 2a. This study remains preliminary and should be extended to a larger sample series (in process).

Altogether, these data obtained by analyzing the expression of ER $\alpha$ 46 in a panel of 116 ER $\alpha$ -positive breast tumors highlights the fact that ER $\alpha$ 46 was expressed in more than 70% of cases. Furthermore, although the expression of this short isoform was highly variable, it correlated with the tumor evolution stage with a higher expression in low-grade tumors and lower expression in tumors that were larger, less differentiated, and of higher-grade.

#### Identification of the ER $\alpha$ 46 isoform

Although the bands observed by Western blot analysis were of the expected sizes, we wanted to confirm the nature of the detected proteins. To reach this aim, we purified the ER $\alpha$  proteins from MCF7 cells and from lysates of four tumor samples by immunoprecipitating the two ER $\alpha$  isoforms using the anti-human ER $\alpha$  primary HC20 antibody (Additional file 1: Figure S4A). After separation by SDS-PAGE, the gel bands corresponding to the 46-kDa and 66-kDa proteins were excised and further digested for proteomic analysis. In MCF7 cells (Table 1), 24.4% of the ER $\alpha$ 66 sequence was covered, including a peptide in the N-terminal domain of amino acids 9–32. Importantly, and as expected, although 23.3% of the ER $\alpha$ 46 sequence was detected, no peptide from the N-terminal A/B domain was identified. Proteomic analysis of immunoprecipitated ER $\alpha$  proteins from four tumor samples respectively covered 25% of the ER $\alpha$ 66 sequence and 15.3% of the ER $\alpha$ 46 sequence (Additional file 1: Figure S4B and S4C). Again, although peptides 184–206, 402–412, and 450–457 were found in the 46 kDa-sized band, no peptides located before the ATG at codon 174 were detected. The first peptide found is 184-206. Therefore, although we were unable to characterize the start codon of ER $\alpha$ 46, we confirm for the first time that the 46-kDa band identified in Western blot analyses of ER $\alpha$ -positive tumors is without doubt a shorter isoform of ER $\alpha$ .

#### ER $\alpha$ 46 can be expressed following alternative initiation of translation in response to stress

It has already been proposed that an alternative initiation of translation could participate in ER $\alpha$ 46 generation through an IRES and the presence of two other potential initiation codons (AUG174/176) in the mRNA coding sequence for amino acids 2–173 of ER $\alpha$  [16]. In line with this potential mechanism, we were able to detect ER $\alpha$ 46 by Western blot analysis in MDA cells transfected with full-length ER $\alpha$ 66 (Fig. 1b). In order to definitively confirm this hypothesis, we analyzed ER $\alpha$ 46 expression in MDA

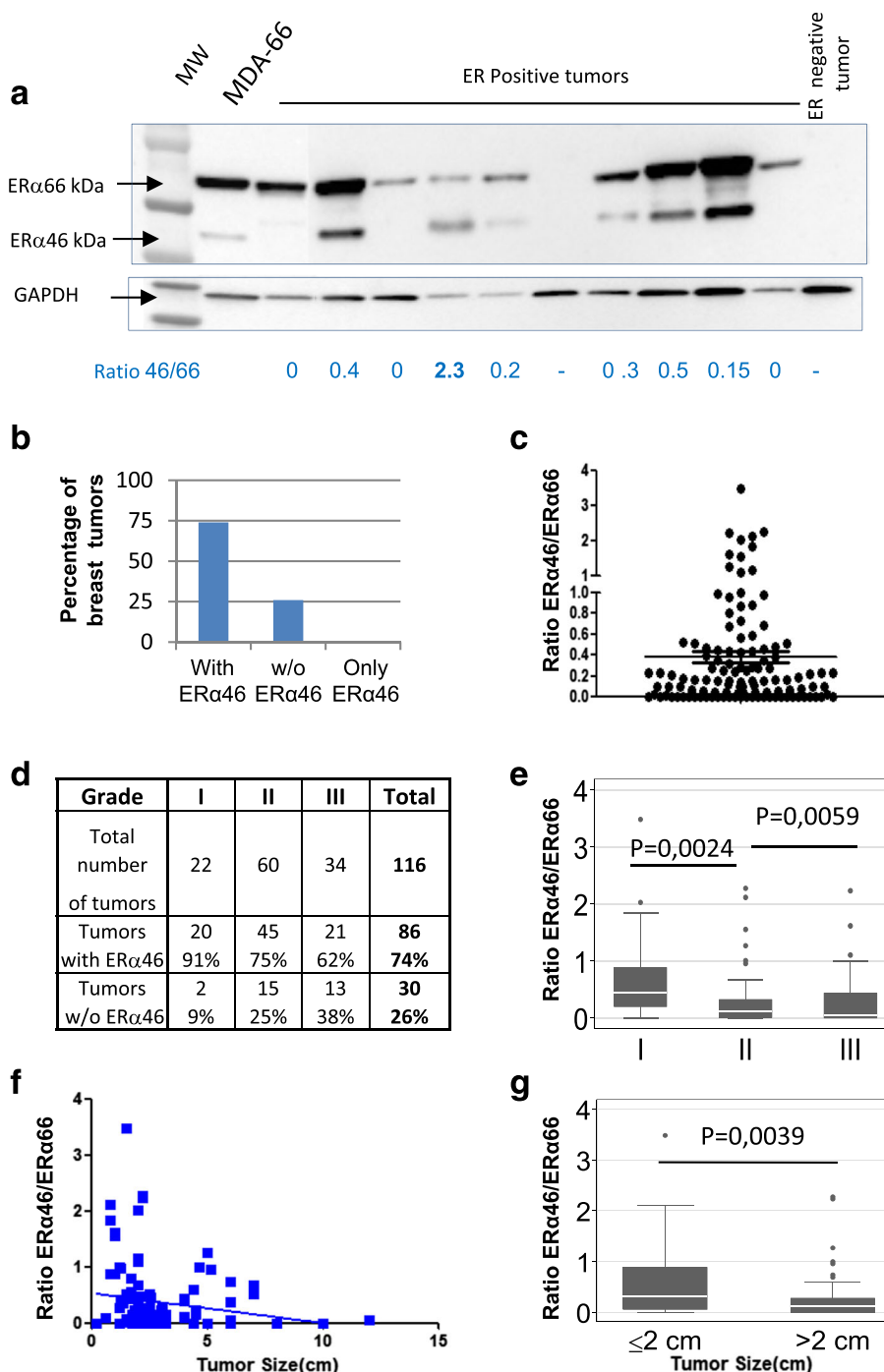


**Fig. 2** Evaluation of the relative expression of estrogen receptor alpha (*ERα*)46 and *ERα*66 in human *ERα*-positive breast tumors. **a** Representative image of Western blot of human *ERα*-positive breast tumor samples blotted with an anti-*ERα* antibody (SP1). One result representative of an *ERα*-negative tumor is also shown. The MDA-*ERα*66 cell line that co-expresses *ERα*66 and *ERα*46 was used as a positive control. The *ERα*46/*ERα*66 expression ratio is indicated below each lane. **b** The summarized data expressed as percentages of tumors expressing *ERα*46 or not. **c** Distribution of the *ERα*46/*ERα*66 expression ratio among the 116 tumor samples. **d** The number and grade of tumors expressing *ERα*46. **e** The *ERα*46/*ERα*66 expression ratio depending upon tumor grade (I, II, or III). **f, g** The *ERα*46/*ERα*66 expression ratio in correlation to tumor size. The whiskers in the boxplots indicate the 10–25% and 75–90% intervals



**Table 1** Proteomic analysis of the 46-kDa protein detected in tumor samples

Tumor	Sample	Mascot score	Cov. (%) / isoform	No. of identified peptides	First N-terminal peptide identified and validated	Peptide identified before Met 174	Last C-terminal peptide identified and validated
MCF7	IP46	759	23.3	14	212–231	No	556–581
	IP66	440	24.4	12	009–032	Yes	556–581
Tumor 1	IP46	96	8.0	5	402–412	No	556–581
	IP66	52	4.4	1	556–581	No	556–581
Tumor 2	IP 46	228	15.3	5	184–206	No	556–581
	IP 66	522	25.0	10	38–48	Yes	556–581
Tumor 3	IP 46	65	3.0	1	450–467	No	450–467
Tumor 4	IP 46	35	1.8	1	402–412	No	402–412

Proteomic analysis results from the different cell lines and the four breast tumor samples

The % of sequence coverage corresponds to the number of amino acid residues identified in the proteomic analysis divided by the total number of amino acid residues in the protein sequence. The Mascot score is described in [52]. It uses statistical methods to assess the validity of a match. This enables a simple rule to be used to judge whether a result is significant or not. We report scores as  $-10 \cdot \log_{10}(P)$ , where P is the absolute probability. A probability of  $10^{-20}$  thus becomes a score of 200

cells transfected with an ER $\alpha$ 46 construct in which the two potential initiation codons of ER $\alpha$ 46 (AUG174/176) were mutated (ER $\alpha$ 46<sup>0</sup>). As shown in Fig. 3a, ER $\alpha$ 46 expression was not detected using this ER $\alpha$ 46<sup>0</sup> construct, demonstrating that the two potential initiation codons are necessary to generate the ER $\alpha$ 46 isoform.

We next sought to determine how this putative IRES sequence can be stimulated. IRESs were found to be activated in tumor cells continually subjected to diverse stress conditions of the tumor microenvironment [32, 33]. Furthermore, accumulating evidence argues for the presence of chronic stress of endoplasmic reticulum or unfolded

protein response (UPR) in different types of cancers, including breast cancer (for a recent review, see [34]). Given the preferential shift towards cap-independent mRNA translation during UPR [35], we hypothesized that endoplasmic reticulum stress might stimulate the translation of open-reading frames downstream of the major initiation codon. To address this question, we transduced MDA-MB-231 cells with a bi-cistronic lentivector carrying the cDNA sequence of the A/B domain (amino acids 2–173) of ER $\alpha$  cloned between LucR and LucF (Fig. 3b). In these transduced MDA cells (Fig. 3c) as well as in transduced MCF7 cells (Additional file 1: Figure S5A), the LucF/LucR ratios

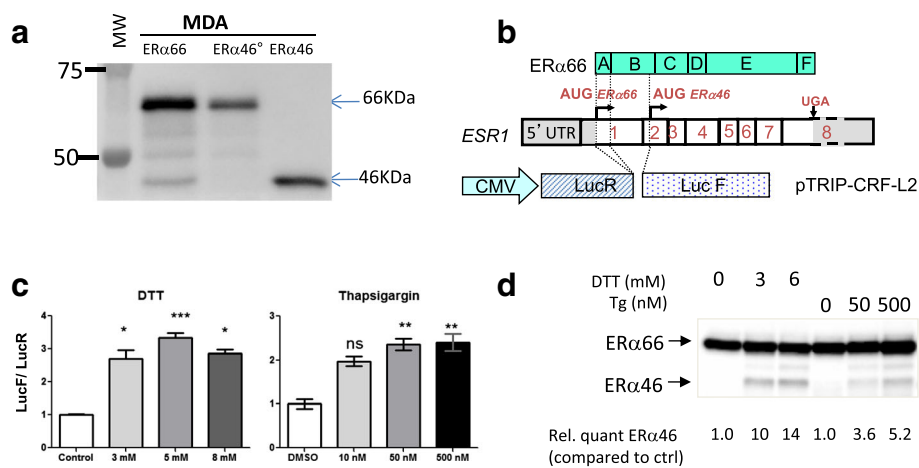


**Fig. 3** IRES-mediated generation of estrogen receptor alpha (ER $\alpha$ )46. **a** A representative image of a Western blot of extracts from MDA-MB-231 cells transfected with constructs expressing either ER $\alpha$ 46, wild-type ER $\alpha$ 66, or an ER $\alpha$ 66 cDNA harboring mutated ATG174/176 codons (ER $\alpha$ 46<sup>0</sup>), illustrating the loss of expression of ER $\alpha$ 46 in cells transfected with the vector encoding ER $\alpha$ 46<sup>0</sup>. **b** Scheme illustrating the bi-cistronic pTRIP-hER $\alpha$ AB-L2 vector harboring the Renilla luciferase (LucR) and Firefly luciferase (LucF(2CP)) cistrons separated by the sequence coding for the A/B domains of the human ER $\alpha$ 66. **c, d** Stress-induced alternative initiation of translation. **c** MDA-MB-231 cells transfected with lentivirus expressing the LucR-hER $\alpha$ AB-LucF construct were subjected to 6 h of stress with 1,4-dithiothreitol (DTT; 3, 5, or 8 mM), thapsigargin (Tg; 10, 50, or 500 nM) or vehicle control (ctrl). Reporter gene activities from three independent experiments in duplicates are shown as the LucF/LucR ratio. **d** Representative Western blot of the increased expression of ER $\alpha$ 46 observed in stressed MDA-MB-231 cells transfected with cDNA expressing ER $\alpha$ 66. \* $P < 0.05$ , \*\* $P < 0.01$ , \*\*\* $P < 0.001$ , versus control (Kruskal-Wallis) ns not significant

were found to be significantly increased in response to UPR inducers (i.e., DTT and thapsigargin) (Fig. 3c). These inductions correlated with the observed increase in ER $\alpha$ 46 protein levels after stress induction in cells stably transfected with the full-length *ESR1* cDNA (Fig. 3d). As a control, we used siRNA directed against LucR which diminished LucF activity (Additional file 1: Figure S5B and C), demonstrating the absence of either an internal promoter in the intervening sequence or stress-induced cryptic alternative splicing that could have shunted the LucR cistron. Taken together, these data suggest that ER $\alpha$ 46 can be produced by stress inducers via an IRES-dependent mechanism.

#### ER $\alpha$ 46 antagonizes the ER $\alpha$ 66-mediated proliferative response of MCF-7 cells to E2 in a dose-dependent manner

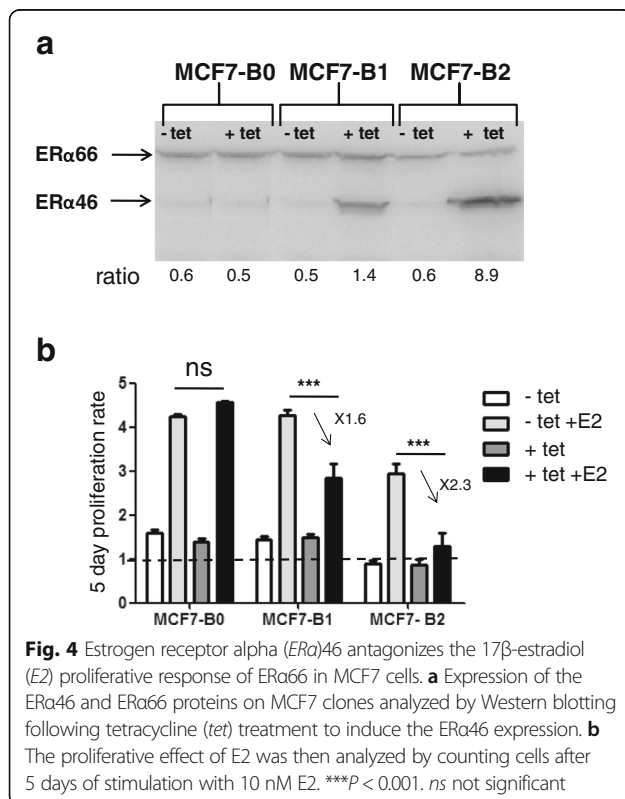
Next, we explored the impact of a high expression level of ER $\alpha$ 46 on E2-induced proliferation of breast tumor cells using MCF-7 cell lines which were engineered to overexpress a tet-inducible ER $\alpha$ 46 (Fig. 4). Proliferation in response to E2 is not influenced by tetracycline treatment as demonstrated using MCF7-B0 sub-clone which expresses an empty vector. By contrast, the proliferation in response to E2 is partially abrogated in the MCF-B1 clone after tetracycline induction (ratio of ER $\alpha$ 46/66 close to 1) and almost completely abolished using the MCF7-B2 clone (ratio of ER $\alpha$ 46/66 close to 10) which expresses the highest expression level of ER $\alpha$ 46. These results indicate that overexpression of the ER $\alpha$ 46 isoform inhibited the E2-

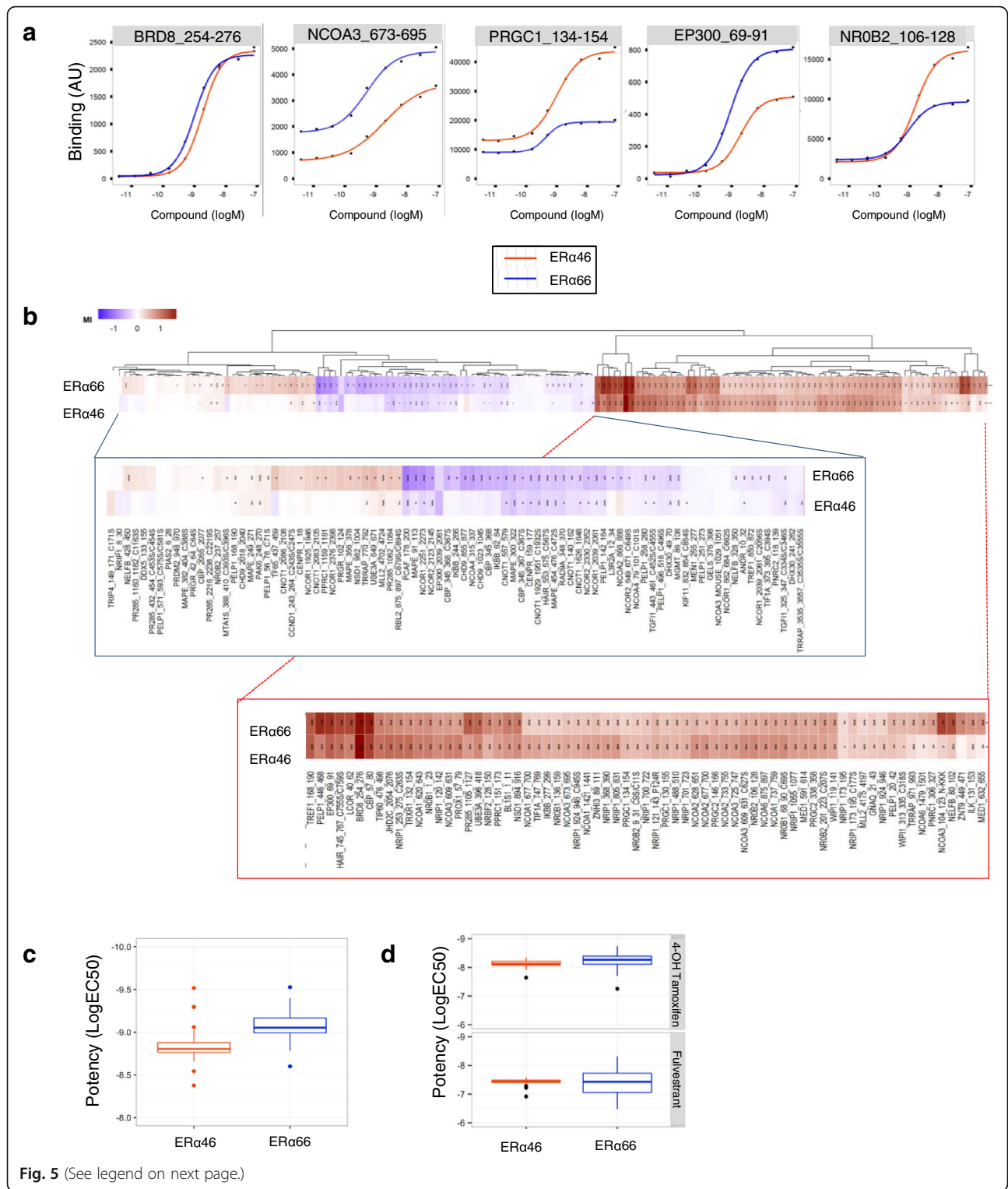
mediated cell proliferation, with inhibition being proportional to the expression of ER $\alpha$ 46.

#### Identification of cofactors that differentially interact with ER $\alpha$ 66 and ER $\alpha$ 46

This inhibition of proliferation may occur through the differential recruitment of coregulators by the ER $\alpha$ 46 and ER $\alpha$ 66 isoforms in the cellular responses induced by E2. To test this hypothesis, we used the MARCoNI assay to characterize the interaction of the two ER $\alpha$  isoforms with 154 unique coregulator-derived motifs, both in their unliganded (apo) conformation or with concentrations of E2 ranging from  $10^{-12}$  to  $10^{-7}$  M, corresponding to full ligand saturation and receptor activation [26]. The resulting overall binding patterns (Additional file 1: Figure S6A and B) indicated that, qualitatively, the receptors bind to the same subset of coregulators, with a clear response of the ER $\alpha$ 46 isoform to E2. However, an isoform-selective difference in the binding affinities of both apo and fully-activated receptors was also observed (Fig. 5a). Further analysis of the E2 response curves evidenced that: (i) both isoforms behave similarly for some interactions (with BRD8 for instance); (ii) some peptides bind better to one of the isoforms, for example NCOA3 (also named SRC-3) which has a higher affinity for ER $\alpha$ 66 and PRGC1 to ER $\alpha$ 46; and (iii) some cofactors bind to both isoforms equally in their apo conformation, but increasing E2 concentrations favor their association with one or the other, as observed for the binding of EP300 to ER $\alpha$ 66 or NROB2 to ER $\alpha$ 46 (Fig. 5a). The hierarchical clustering of ligand-induced modulation of coregulator interactions was then performed to look for differences and was quantified as the log-fold change in binding (modulation index (MI)) (Fig. 5b). This analysis confirmed that, although qualitatively the overall responses looked generally quite similar, there is a quantitative differential modulation with some selective preference to certain coregulator peptides. Upon E2 binding, an overall increased preference for cofactor binding to ER $\alpha$ 66 over ER $\alpha$ 46 was observed, as shown in Fig. 5c.

We then investigated the potency of the ER $\alpha$  antagonists 4-OH-tamoxifen and fulvestrant in inhibiting cofactor binding to ER $\alpha$ 46 and ER $\alpha$ 66 in the presence of E2. The profile of the EC $_{50}$  values for 4-OH-tamoxifen and fulvestrant clearly showed a better efficacy of 4-OH-tamoxifen than fulvestrant in inhibiting E2-induced binding of the receptor isoforms to coregulators (Additional file 1: Figure 6C). However, the potencies of these antagonists to inhibit binding to ER $\alpha$ 46 and ER $\alpha$ 66 were comparable (Fig. 5d). Altogether, these data clearly demonstrate that the two isoforms show some specificity and heterogeneity in terms of their binding to coregulators.





(See figure on previous page.)

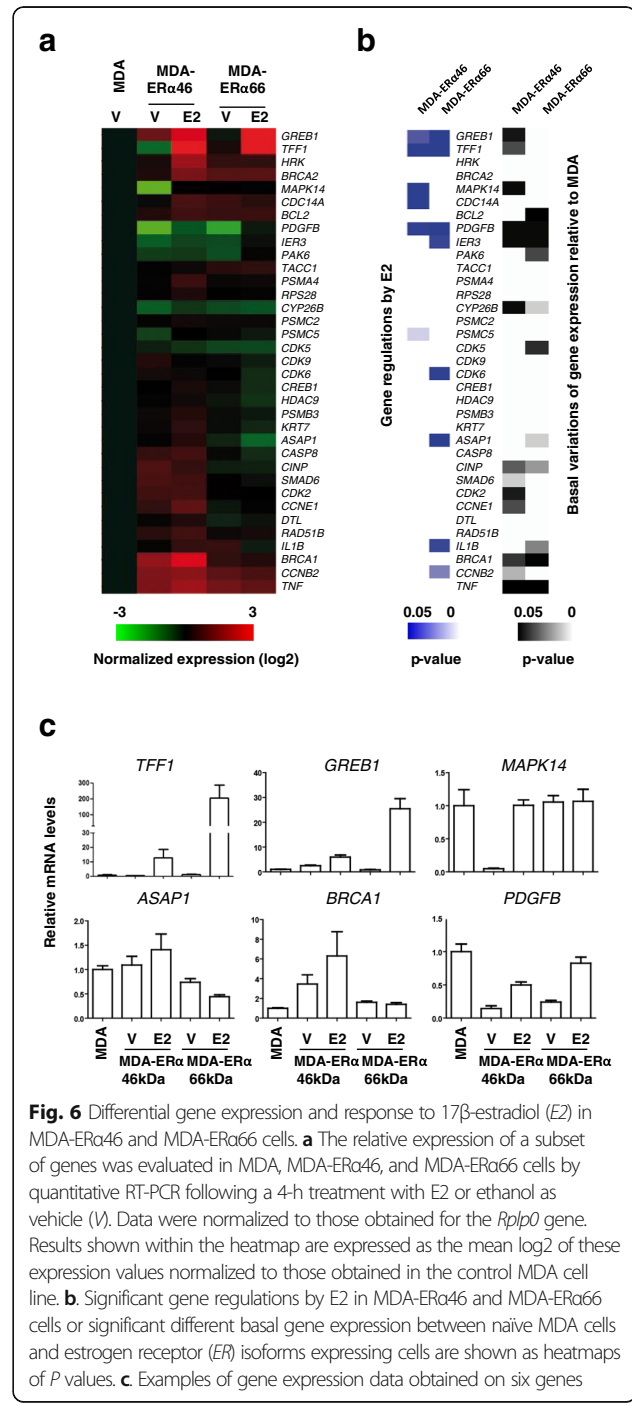
**Fig. 5** Ligand-specific coregulator binding profiles. Interactions of the estrogen receptor alpha (ERα)46 and ERα66 proteins with coregulator motifs were measured using MARCoNI peptide arrays. Interactions were evaluated at different concentrations of E2, ranging from 10<sup>-12</sup> to 10<sup>-7</sup> M. **a** Examples of dose-dependent E2-mediated modulation of ERα46 and ERα66 interactions with individual coregulator motifs to illustrate that the two proteins bind to coregulators with differential affinities. **b** Heatmap showing hierarchical clustering (Euclidean distance, average linkage) of E2-mediated interactions (represented as the modulation index (MI)) between ERα46 and ERα66 proteins and peptides representing coregulator-derived binding motifs. MI is expressed as log of fold changes relative to vehicle. Zoom outs from the left and the right main clusters are shown below. **c** Boxplot representation of E2 potency for the modulation of coregulator binding of the two isoforms, using EC<sub>50</sub> values obtained with the curve fit R<sup>2</sup> > 0.8. **d** Mean of all EC<sub>50</sub> (logM) values of the ability of fulvestrant and 4-OH-tamoxifen to modulate fully E2-activated coregulator binding to either ERα46 or ERα66

### Differential gene expression response to E2 mediated by ERα46 and ERα66

In order to evaluate the impact of differences in coregulator affinity between the two ERα isoforms in terms of transcriptional regulation, we aimed at determining the expression of some target genes in MDA-ERα46 and MDA-ERα66 cells in response to E2. To directly assess the correlation between these events and cell proliferation, we selected a set of genes for their known association with this process, some of them also described as regulated by E2 in MCF7 breast cancer cells or MDA-ERα66 cells (Additional file 1: Figure S7) [36, 37]. The data (Fig. 6 and Additional file 1: Figure S8) indicate that the majority of the tested genes are differentially regulated in MDA-ERα46 and MDA-ERα66 cells. While some genes were found to be regulated by E2 in MDA cells expressing either ERα66 or ERα46, albeit at higher levels for the ERα66 (*GREB1*, *TFF1*, and *PDGFB*), some genes were specifically regulated by the ERα46 (*MAPK14* and *CDC14A*) or the ERα66 (*IER3*, *CDK6*, *ASAP1*, *IL1B*, and *CCNB2*). Moreover, the basal levels of transcription were also differentially affected by the expression of these isoforms as compared to naïve MDAwt cells. Indeed, some genes were specifically affected by either the ERα66 (*CDK5* and *IL1B*), or the ERα46 (*GREB1*, *TFF1*, *MAPK14*, *CDK2*, and *CCNE1*) but also by both isoforms (*PDGFB*, *IER3*, *BRCA1*, and *TNF*). Altogether, these data clearly demonstrate that ERα46 and ERα66 have different transcriptional activities.

### Discussion

The work reported here aimed to analyze the expression levels and characteristics of the overlooked ERα46 isoform in breast tumor samples. We have clearly shown that ERα46 is expressed in the majority of human breast tumors tested (more than 70%) with highly variable expression levels, sometimes even more abundant than ERα66. Importantly, the ERα46/ERα66 expression ratio negatively correlated with tumor grade: poorly-differentiated tumors (of higher grade and larger size) presented lower amounts of ERα46. These data indicate that this shorter isoform may have a potential clinical relevance. Unfortunately, since this retrospective study started in 2011, it is too early to further analyze any correlation between the abundance of ERα46 and overall survival or recurrence of disease.





This criterion requires a time period of 15–20 years due to delayed tumor relapses of ER $\alpha$ -positive tumors [38].

A previous study reported the expression of a 47-kDa isoform in human breast cancer that is able to bind to radioactive tamoxifen aziridine, which could be the same as the 46-kDa ER $\alpha$  isoform described here [20]. Using electrophoresis with radiolabeled tamoxifen, the authors found that 49% of tumor samples to express the 67- and the 47-kDa protein entities, whereas 36% contained only the longest form. Our proteomic analysis is the first to definitively identify the band detected by Western blot as an ER $\alpha$  isoform deprived of the A/B domain.

Our results also show that several of the antibodies currently used for the diagnosis of breast cancer are unable to detect the ER $\alpha$ 46 isoform. Indeed, the 1D5, 6 F11, and EP1 antibodies are directed against the A/B domain, which is absent in ER $\alpha$ 46 (Fig. 6). As a consequence, the hormone-dependent characterization of the tumor, presently performed by immunohistochemistry, may only be based on the expression level of ER $\alpha$ 66. This finding highlights the importance of the choice of antibodies used for the diagnosis of breast cancer, which able or not to detect the ER $\alpha$ 46 isoform.

Furthermore, we found that ER $\alpha$ 46 expression level was related to tumor size, suggesting that expression of the 46-kDa isoform in breast tumors could be associated with a limited tumor growth. Such a hypothesis is supported by previous studies demonstrating that ER $\alpha$ 46 antagonizes the proliferative effects induced by ER $\alpha$ 66 activation both in vitro in MCF7 cells [17] and SaOS osteosarcoma cells [9], as well as in colorectal tumor tissues [12]. Its expression could therefore maintain a low tumor volume, possibly by stimulating apoptosis [12]. We confirmed these data and also found that increasing the amount of ER $\alpha$ 46 in MCF7 cells decreases their proliferative response to E2 in a dose-dependent manner. Importantly, other studies have linked the N-terminal region of ER $\alpha$  with cell proliferation. Merot et al. [39] used in vitro systems to show that the respective contribution of AF-1 and AF-2 towards ER $\alpha$  transcriptional activity varies upon the stage of cell differentiation. This key role of AF-1 was also demonstrated physiologically in the uterus, a tissue that is highly sensitive to the proliferative actions of E2 in vivo. Indeed, it was shown that E2 had no proliferative action on uterine epithelial cells in ER $\alpha$ -AF1<sup>0</sup> mice, which express an AF-1-deficient 49-kDa ER $\alpha$  isoform [19]. ER $\alpha$  has been described as being at the crossroads of paracrine or autocrine growth factor and endocrine estrogenic signaling [40], and its activity can be controlled in the absence of E2 through phosphorylation cascades induced by insulin-like growth factor (IGF)-1, epidermal growth factor (EGF), or fibroblast growth factor (FGF)-2. Importantly, most of the residues of ER $\alpha$  that have so far been implicated in these E2-independent responses or in the modulation of ER $\alpha$  activities in response to growth factor signaling are located

within the N-terminal region of the protein and constitute an intrinsic part of AF-1 [41]. Altogether, these data support the hypothesis that AF-1 is the region of ER $\alpha$  required for cell proliferation, and that its absence in the ER $\alpha$ 46 isoform is likely to confer specific properties to this protein compared to the ER $\alpha$ 66 isoform.

In our study, we also analyzed the ability of the two isoforms to bind cofactors using the MARCoNI assay, and found that the two isoforms show some heterogeneity in terms of binding to coregulators. The ability of the two apo-ER $\alpha$  isoforms to recruit transcription factors to the *pS2/TFF1* promoter was previously compared by Re-ChIP experiments [22]. This study identified that ER $\alpha$ 46 specifically recruited components of the Sin3 repressive complex (NCOR/SMRT) to the *TFF1* promoter in the absence of E2. This was associated with specific inhibition of the basal transcription of the *TFF1* gene by the ER $\alpha$ 46 isoform. More recently, the quaternary structure of a biologically active ER $\alpha$ -coactivator complex on DNA has been determined by cryoelectron microscopy [42]. This study showed the location of the AF-1 domain in the complex, which supports a role in the recruitment of the coactivator SRC-3. Interestingly, in our assay we also found a stronger binding of ER $\alpha$ 66 to some peptides derived from SRC-3 (Fig. 5b). In contrast, the ER $\alpha$ 46 isoform was found to bind to NRB02 better than the ER $\alpha$ 66 isoform. NRB02 acts as a negative regulator of receptor-dependent signaling pathways [43]. These data therefore underline the importance of the AF-1 domain for full transcriptional activation of the ER $\alpha$ -coactivator complex. Indeed, our study also demonstrates a differential gene expression induced by ER $\alpha$ 46 or ER $\alpha$ 66 at the basal level but also in response to E2. Interestingly, among these differentially regulated genes, ER $\alpha$ 46 specifically upregulated the *MAPK14* and *CDC14* genes in the presence of E2 (respectively 20- and 1.7-fold) as opposed to the ER $\alpha$ 66 isoform. These genes are implicated in the suppression of the cell proliferation [44, 45] and these regulations may at least partly explain the reduced E2-mediated proliferative response observed when ER $\alpha$ 46 is co-expressed. Although not significant, the originally identified proapoptotic *HRK* gene [46] also exhibited a slight tendency to be specifically regulated by the ER $\alpha$ 46 (twofold,  $P = 0.09$ ).

Our observations raise the hypothesis that the presence of the short ER $\alpha$ 46 isoform in breast tumors could indicate a more favorable prognosis. Such an assessment is also supported by the study of Klinge et al. who indicated that almost 40% of patients developing a secondary tamoxifen resistance exhibit a reduced expression of ER $\alpha$ 46 [13]. This supports the idea that endocrine resistance is associated with a decreased expression of ER $\alpha$ 46 and thus with poor breast cancer prognosis. Subtle interactions between these isoforms could influence the action of selective estrogen receptor modulators (SERMs) against tumor growth and metastasis. Interestingly, tamoxifen antagonizes the AF-2



of both the ER $\alpha$ 66 and ER $\alpha$ 46 isoforms, but at the same time acts as an agonist on AF-1 of ER $\alpha$ 66 in a tissue-dependent manner. Due to the lack of AF-1, tamoxifen cannot elicit such an action on ER $\alpha$ 46. As shown in our analysis with the MARCoNI assay, ER $\alpha$ 46 appears to be as potent as the ER $\alpha$ 66 in dissociating coregulatory binding in response to tamoxifen or fulvestrant. However, since these interactions are very complex, further investigations are needed in tumor samples *in vivo*.

Altogether, these data point out the importance of the expression of both ER $\alpha$  isoforms in breast tumors. In the absence of an ER $\alpha$ 46-specific antibody, automated immunoblot analyses would be necessary to render ER $\alpha$ 46 detection practically feasible in breast cancer diagnosis. However, it cannot be ruled out that new techniques based on structural

properties of the two estrogen receptors could appear in the future [47]. Further characterization of ER $\alpha$ 46 will then be needed to refine both prognosis and therapy. Although the exact mechanisms accounting for the expression of the ER $\alpha$ 46 isoform still remain to be clarified, three potential processes have been identified: (i) alternative splicing could generate an mRNA deficient in the nucleotide sequence corresponding to exon 1 encoding the A/B domain [14]; (ii) proteolysis, as has also been suggested in human breast tumors [15] and in the mouse uterus [48]; and (iii) an IRES located within the full length mRNA could allow the initiation of translation at a downstream ATG which encodes methionine 174 in the human ER $\alpha$ 66 [16] (Fig. 7). Unfortunately, our proteomic approach did not identify peptides close to this initiation codon. One potential explanation for this is

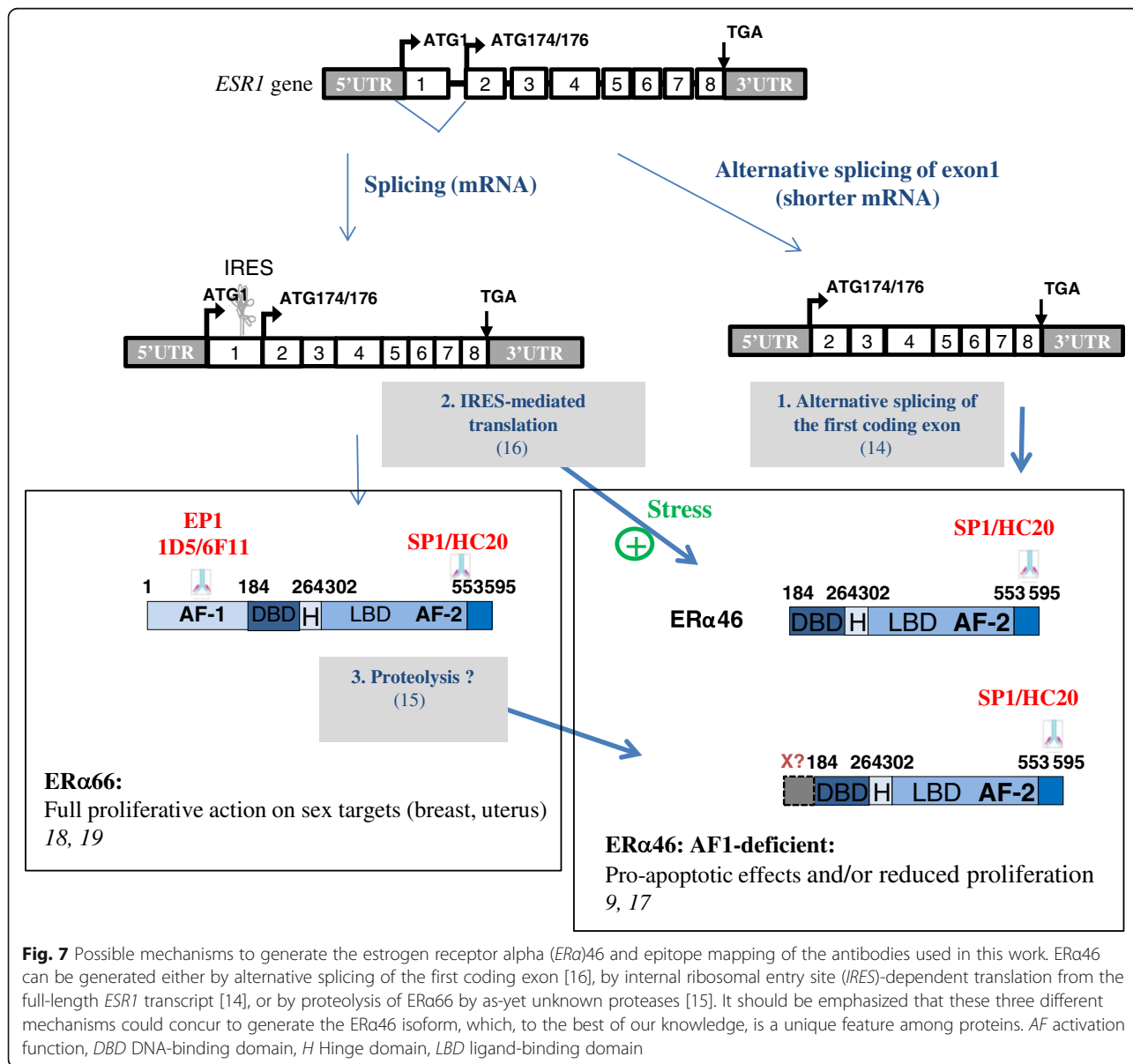


**Fig. 7** Possible mechanisms to generate the estrogen receptor alpha (ER $\alpha$ )46 and epitope mapping of the antibodies used in this work. ER $\alpha$ 46 can be generated either by alternative splicing of the first coding exon [16], by internal ribosomal entry site (IRES)-dependent translation from the full-length *ESR1* transcript [14], or by proteolysis of ER $\alpha$ 66 by as-yet unknown proteases [15]. It should be emphasized that these three different mechanisms could concur to generate the ER $\alpha$ 46 isoform, which, to the best of our knowledge, is a unique feature among proteins. AF activation function, DBD DNA-binding domain, H Hinge domain, LBD ligand-binding domain

the presence of lysine and arginine residues (target residues for trypsin) in the vicinity to the two potential initiation codons (KGSMAMESAKETRY). The length of the peptides generated after complete trypsin digestion may be too short to be identified despite the high dynamic range of the nano-LC-MS/MS system used for the proteomic analysis. At this stage, it is not possible to determine the respective roles of the different mechanisms of ER $\alpha$ 46 generation. However, we provide evidence that an IRES-dependent alternative translational initiation under stress conditions could lead to the generation of ER $\alpha$ 46. This is further supported by the association of the ER $\alpha$  mRNA, along with other IRES-containing mRNAs, to polysomes in apoptotic MCF7 cells in which cap-dependent translation is repressed [49]. Moreover, 4E-BP1, a negative regulator of cap-dependent mRNA translation, was found to be overexpressed in breast tumors compared to healthy epithelium, suggesting that translational mechanisms such as IRES might be active [50]. Interestingly, genes such as Apaf-1, DAP5, CHOP, p53, etc., that are also selectively translated by an IRES-driven mechanism, allow the cells to fine-tune their responses to cellular stress and, if conditions for cell survival are not restored, to proceed with final execution of apoptosis [51]. Although the significance of induction of ER $\alpha$ 46 by cellular stress remains unknown, this isoform of ER $\alpha$  could be part of an orchestrated IRES-driven response, and contribute to slowing down of the proliferative response to E2.

## Conclusions

This study demonstrates that a shorter ER $\alpha$ 46 isoform previously ignored in diagnosis is frequently expressed in ER $\alpha$ -positive breast tumors, as revealed by Western blot analysis. Careful attention should therefore be taken in the choice of antibodies used for immunohistochemistry as several do not detect the expression of the ER $\alpha$ 46 isoform. We have demonstrated that this shorter isoform can differentially bind to coregulators in response to E2 which might modulate the transcriptional hormonal response. This highlights the potential importance of this shorter isoform in E2 signaling and its antiproliferative actions in breast cancer. We indeed found a clear inverse correlation between tumor size and ER $\alpha$ 46 levels. Thus, due to the importance of ER $\alpha$  and hormonal treatments in the management of breast cancers, ER $\alpha$ 46 expression should now be further studied.

## Additional file

**Additional file 1: Figure S1.** Clinical parameters of the breast tumor samples. *IDC* invasive ductal carcinoma, *ILC* invasive lobular carcinoma. **Figure S2.** Expression of Flag-ER $\alpha$ 36 in transiently transfected MDA-MB231 as detected by immunocytochemistry using an anti-Flag antibody. **Figure S3.** Analysis of potential correlation between the clinical parameters of the breast tumor samples and the expression of ER $\alpha$ 46 isoform. A significant *P* value (indicated in red) was only found between ER $\alpha$ 46 expression and HER-2 positive breast tumors. *IDC* invasive ductal carcinoma,

*ILC* invasive Lobular Carcinoma. **Figure S4.** Results of the proteomic analysis of the ER $\alpha$ 46 protein detected in tumor samples. A) Western blot with the SP1 antibody obtained after immunoprecipitation of ER $\alpha$  with HC20 antibody in two human tumors overexpressing the putative ER $\alpha$ 46 isoform. B and C) Sequence coverage obtained from the peptides identified by proteomic analysis shown in bold red on ER $\alpha$ 66 and on ER $\alpha$ 46 isoforms M (methionine); putative translational start sites generating the ER $\alpha$ 46 isoform. **Figure S5.** The stress-induced increase in LucF activity is reproducible in MCF7 cells (A) and is not due to the generation of mono-cistronic LucF transcripts via an internal promoter or cryptic splicing as observed in MDA-Lenti-AB exposed to two siRNAs-lucR (B and C). **Figure S6.** Modulation profiles of the interaction of ER $\alpha$ 46 (red) and ER $\alpha$ 66 (blue) with coregulators in A) Apo proteins and B) in response to E2 binding. C) Profile of EC<sub>50</sub> values of 4-OH-tamoxifen (red) and fulvestrant (blue) induced modulation of ER $\alpha$ 46 and ER $\alpha$ 66 coregulators interaction when use in antagonists mode with 6.3 nM E2. **Figure S7.** List of primers used in the expression profiling of target genes. **Figure S8.** Fold-changes (FC) in gene expression  $\pm$  SEM in MDA-ER $\alpha$ 46 and MDA-ER $\alpha$ 66 cells in response to 4-h treatment with E2 (10<sup>-8</sup> M). *P* values were determined by Mann-Whitney test. Significant *P* values are indicated in red. (PPTX 939 kb)

## Abbreviations

AF-1: Activation function 1; AJCC: American Joint Committee on Cancer; ChIP: Chromatin immunoprecipitation; DMEM: Dulbecco's modified Eagle's medium; DTT: 1,4-Dithiothreitol; E2: 17 $\beta$ -estradiol; ECL: Enhanced chemiluminescence; EDTA: Ethylenediaminetetraacetic acid; EGF: Epidermal growth factor; ER: Estrogen receptor; ERE: Estrogen responsive element; FCS: Fetal calf serum; FGF: Fibroblast growth factor; HER2: Human epidermal growth factor receptor-2; HRP: Horseradish peroxidase; IGF: Insulin-like growth factor; IRES: Internal ribosomal entry site; LC-MS/MS: Liquid chromatography coupled to tandem mass spectrometry; LucF: Firefly luciferase; LucR: Renilla luciferase; MARCoNI: Microarray Assay for Real-time Coregulator-Nuclear receptor Interaction; PBS: Phosphate-buffered saline; PCR: Polymerase chain reaction; RT: Reverse transcription; SERM: Selective estrogen receptor modulator; UPR: Unfolded protein response

## Acknowledgements

We particularly thank the staff of the Institut Universitaire du Cancer Toulouse – Oncopole and the University Hospital Rangueil in Toulouse, France, particularly Prof. Pierre Leguevaque, Dr. Charlotte Vaysse, and Dr. Guylaine Escourrou, who helped us to collect the breast tumor samples, Armelle Gaston, Audrey Benest, and Loubna M'Hamdi who performed the immunohistochemistry on tumor cell lines and breast biopsies, and Christelle Casaroli and Laurence Puydenus who helped us to collect all the clinical parameters of the patients. We also thank Dr. Barbara Garmy-Susini (INSERM U1048, Toulouse, France) for fruitful discussions and comments on the manuscript.

## Funding

The work at the INSERM U1048 is supported by INSERM, Université Toulouse III, and the Faculté de Médecine Toulouse-Rangueil, the Agence Nationale de la Recherche ANR N°-14-CE12-0021-01, the Conseil Régional Midi-Pyrénées, the Fondation pour la Recherche Médicale, the Fondation de France and La Ligue Contre le Cancer. EC was supported by a grant from the CHU Rangueil Toulouse. The work at IPBS was supported in part by the Région Midi Pyrénées, the Toulouse Métropole and European funds (FEDER). Work at the IGDR in Rennes was supported by the CNRS and the University of Rennes 1 as well as from fundings of the ARC.

## Availability of data and materials

The data concerning the tumor samples that support the findings of this study cannot be shared in a public repository according to the CNIL (Comité National Informatique et Libertés) guidelines. The other datasets used and/or analyzed during the current study are available from the corresponding author on reasonable request.

## Authors' contributions

FL was the principal investigator who conceived, coordinated, oversaw the study, and wrote the manuscript. JFA and CF helped in the study design and in writing the manuscript. EC, FB, and HL acquired, analyzed, interpreted the experiment data, and helped to revise the manuscript. AS and OBS acquired the data of the proteomics analysis and helped to revise the manuscript. RM

and GP acquired the data of the transcriptional response and helped to draft the manuscript. GF performed the experiments on the proliferative response in MCF7 cells and helped to revise the manuscript. DM and RH performed all the analysis of the coregulator binding analysis and helped to draft the manuscript. TF was responsible for statistical analysis and helped to revise the manuscript. EC, PR, and AB participated in the preparation of the biological samples and helped to revise the manuscript. All authors read and approved the final manuscript.

#### Competing interests

The authors declare that they have no competing interests.

#### Consent for publication

Not applicable.

#### Ethics approval and consent to participate

Breast tumor samples were obtained from the "CRB cancer des Hôpitaux de Toulouse; BB-0033-00014; BC-2016-2656 and AC-2016-2658" collection and was approved by the Institutional and National ethics committees. Patient samples were obtained after authorization by the French Ministry of Higher Education and Research (declaration DC 2009-989; DC-2011-1388; transfer agreement AC-2008-820; AC-2011-130) and from the "Comité de Protection des Personnes Sud Ouest et Outre Mer- l'Agence Régionale de Santé Midi-Pyrénées, Toulouse". Clinical and biological annotations were consistent with the CNIL (Comité National Informatique et Libertés) guidelines (see Additional file 1: Figure S1 for clinical parameters of the patients used).

#### Author details

<sup>1</sup>INSERM U1048, Institut des Maladies Métaboliques et Cardiovasculaires, Université de Toulouse, BP 84225, 31 432 Toulouse cedex 04, France. <sup>2</sup>Pôle IUC Oncopole CHU, Institut Universitaire du Cancer de Toulouse - Oncopole, 1 avenue Irène Joliot-Curie, 31059 Toulouse cedex 9, France. <sup>3</sup>UMR CNRS 6290, Institut de Génétique et Développement de Rennes, Equipe SP@RTE, Rennes 35042 Cedex, France. <sup>4</sup>PamGene International B.V, P.O. Box 13455200, BJ, 's-Hertogenbosch, The Netherlands. <sup>5</sup>Institut de Pharmacologie et de Biologie Structurale, Université de Toulouse, CNRS, UPS, Toulouse, France. <sup>6</sup>INSERM U1085, IRSET (Institut de Recherche en Santé, Environnement et Travail), Université de Rennes 1, 35000 Rennes, France.

Received: 30 March 2016 Accepted: 12 November 2016

Published online: 07 December 2016

#### References

- Ferlay J, Soerjomataram I, Dikshit R, Eser S, Mathers C, Rebelo M, Parkin DM, Forman D, Bray F. Cancer incidence and mortality worldwide: sources, methods and major patterns in GLOBOCAN 2012. *Int J Cancer*. 2015;136(5):E359–86.
- Johnston SR. New strategies in estrogen receptor-positive breast cancer. *Clin Cancer Res*. 2010;16(7):1979–87.
- Fisher B, Anderson S, Redmond CK, Wolmark N, Wickerham DL, Cronin WM. Reanalysis and results after 12 years of follow-up in a randomized clinical trial comparing total mastectomy with lumpectomy with or without irradiation in the treatment of breast cancer. *N Engl J Med*. 1995;333(22):1456–61.
- Howell A. Adjuvant aromatase inhibitors for breast cancer. *Lancet*. 2005;366(9484):431–3.
- Silvestrini R, Daidone MG, Luisi A, Boracchi P, Mezzetti M, Di Fronzo G, Andreola S, Salvadori B, Veronesi U. Biologic and clinicopathologic factors as indicators of specific relapse types in node-negative breast cancer. *J Clin Oncol*. 1995;13(3):697–704.
- Polyak K, Vogt PK. Progress in breast cancer research. *Proc Natl Acad Sci U S A*. 2012;109(8):2715–7.
- Jordan VC, O'Malley BW. Selective estrogen-receptor modulators and antihormonal resistance in breast cancer. *J Clin Oncol*. 2007;25(36):5815–24.
- Wang Z, Zhang X, Shen P, Loggie BW, Chang Y, Deuel TF. Identification, cloning, and expression of human estrogen receptor-alpha36, a novel variant of human estrogen receptor-alpha66. *Biochem Biophys Res Commun*. 2005;336(4):1023–7.
- Denger S, Reid G, Kos M, Flouriot G, Parsch D, Brand H, Korach KS, Sonntag-Buck V, Gannon F. ERalpha gene expression in human primary osteoblasts: evidence for the expression of two receptor proteins. *Mol Endocrinol*. 2001;15(12):2064–77.
- Murphy AJ, Guyre PM, Wira CR, Pioli PA. Estradiol regulates expression of estrogen receptor ERalpha46 in human macrophages. *PLoS One*. 2009;4(5), e5539.
- Li L, Haynes MP, Bender JR. Plasma membrane localization and function of the estrogen receptor alpha variant (ER46) in human endothelial cells. *Proc Natl Acad Sci U S A*. 2003;100(8):4807–12.
- Jiang HP, Teng RY, Wang Q, Zhang X, Wang HH, Cao J, Teng LS. Estrogen receptor alpha variant ERalpha46 mediates growth inhibition and apoptosis of human HT-29 colon adenocarcinoma cells in the presence of 17beta-estradiol. *Chin Med J (Engl)*. 2008;121(11):1025–31.
- Klinge CM, Riggs KA, Wickramasinghe NS, Emberts CG, McConda DB, Barry PN, Magnusen JE. Estrogen receptor alpha 46 is reduced in tamoxifen resistant breast cancer cells and re-expression inhibits cell proliferation and estrogen receptor alpha 66-regulated target gene transcription. *Mol Cell Endocrinol*. 2010;323(2):268–76.
- Flouriot G, Brand H, Denger S, Metivier R, Kos M, Reid G, Sonntag-Buck V, Gannon F. Identification of a new isoform of the human estrogen receptor-alpha (hER-alpha) that is encoded by distinct transcripts and that is able to repress hER-alpha activation function 1. *Embo J*. 2000;19(17):4688–700.
- Maaroufi Y, Lacroix M, Lespagnard L, Journe F, Larsimont D, Leclercq G. Estrogen receptor of primary breast cancers: evidence for intracellular proteolysis. *Breast Cancer Res*. 2000;2(6):444–54.
- Barraille P, Chinestra P, Bayard F, Faye JC. Alternative initiation of translation accounts for a 67/45 kDa dimorphism of the human estrogen receptor ERalpha. *Biochem Biophys Res Commun*. 1999;257(1):84–8.
- Penot G, Le Peron C, Merot Y, Grimaud-Fanouillere E, Ferriere F, Boujrad N, Kah O, Saligaut C, Ducouret B, Metivier R, et al. The human estrogen receptor-alpha isoform hERalpha46 antagonizes the proliferative influence of hERalpha66 in MCF7 breast cancer cells. *Endocrinology*. 2005;146(12):5474–84.
- Billon-Gales A, Fontaine C, Filipe C, Douin-Echinard V, Fouque MJ, Flouriot G, Gourdy P, Lenfant F, Laurell H, Krust A, et al. The transactivating function 1 of estrogen receptor alpha is dispensable for the vasculoprotective actions of 17beta-estradiol. *Proc Natl Acad Sci U S A*. 2009;106(6):2053–8.
- Abot A, Fontaine C, Raymond-Letron I, Flouriot G, Adlanmerini M, Buscato M, Otto C, Berges H, Laurell H, Gourdy P, et al. The AF-1 activation function of estrogen receptor alpha is necessary and sufficient for uterine epithelial cell proliferation in vivo. *Endocrinology*. 2013;154(6):2222–33.
- Jozan S, Julia AM, Carretie A, Eche N, Maisongrosse V, Fouet B, Marques B, David JF. 65 and 47 kDa forms of estrogen receptor in human breast cancer: relation with estrogen responsiveness. *Breast Cancer Res Treat*. 1991;19(2):103–9.
- Reid G, Hubner MR, Metivier R, Brand H, Denger S, Manu D, Beaudouin J, Ellenberg J, Gannon F. Cyclic, proteasome-mediated turnover of unliganded and liganded ERalpha on responsive promoters is an integral feature of estrogen signaling. *Mol Cell*. 2003;11(3):695–707.
- Metivier R, Penot G, Carmouche RP, Hubner MR, Reid G, Denger S, Manu D, Brand H, Kos M, Benes V, et al. Transcriptional complexes engaged by estrogen receptor-alpha isoforms have divergent outcomes. *Embo J*. 2004;23(18):3653–66.
- Elston CW, Ellis IO. Pathological prognostic factors in breast cancer. I. The value of histological grade in breast cancer: experience from a large study with long term follow up. *Histopathology* 1991;19:403–10.
- Ainaoui N, Hantelys F, Renaud-Gabardos E, Bunel M, Lopez F, Pujol F, Planes R, Bahraoui E, Pichereaux C, Bulet-Schiltz O, et al. Promoter-dependent translation controlled by p54nrb and hnRNP during myoblast differentiation. *PLoS One*. 2015;10(9), e0136466.
- Arvidsson S, Kwasniewski M, Riano-Pachon DM, Mueller-Roeber B. QuantPrime—a flexible tool for reliable high-throughput primer design for quantitative PCR. *BMC Bioinformatics*. 2008;9:465.
- Koppen A, Houtman R, Pijnenburg D, Jennings EH, Ruijtenbeek R, Kalkhoven E. Nuclear receptor-coregulator interaction profiling identifies TRIP3 as a novel peroxisome proliferator-activated receptor gamma cofactor. *Mol Cell Proteomics*. 2009;8(10):2212–26.
- Houtman R, de Leeuw R, Rondaij JM, Melchers D, Verwoerd D, Ruijtenbeek R, Martens JW, Neeffes J, Michalides R. Serine-305 phosphorylation modulates estrogen receptor alpha binding to a coregulator peptide array, with potential application in predicting responses to tamoxifen. *Mol Cancer Ther*. 2012;11(4):805–16.
- al Saati T, Clamens S, Cohen-Knafo E, Faye JC, Prats H, Coindre JM, Wafflard J, Caveriviere P, Bayard F, Delsol G. Production of monoclonal antibodies to human estrogen-receptor protein (ER) using recombinant ER (RER). *Int J Cancer*. 1993;55(4):651–4.

29. Cheang MC, Treaba DO, Speers CH, Olivetto IA, Bajdik CD, Chia SK, Goldstein LC, Gelmon KA, Huntsman D, Gilks CB, et al. Immunohistochemical detection using the new rabbit monoclonal antibody SP1 of estrogen receptor in breast cancer is superior to mouse monoclonal antibody 1D5 in predicting survival. *J Clin Oncol*. 2006;24(36):5637–44.
30. Bogina G, Zamboni G, Sapino A, Bortesi L, Marconi M, Lunardi G, Coati F, Massocco A, Molinaro L, Pegoraro C, et al. Comparison of anti-estrogen receptor antibodies SP1, 6 F11, and 1D5 in breast cancer: lower 1D5 sensitivity but questionable clinical implications. *Am J Clin Pathol*. 2012; 138(5):697–702.
31. Madeira KP, Daltoe RD, Sirtoli GM, Rezende LC, Carvalho AA, Guimaraes Idos S, Silva IV, Rangel LB. Comparison of immunohistochemical analysis with estrogen receptor SP1 and 1D5 monoclonal antibodies in breast cancer. *Pathol Res Pract*. 2012;208(11):657–61.
32. Faye MD, Holcik M. The role of IRES trans-acting factors in carcinogenesis. *Biochim Biophys Acta*. 2015;1849(7):887–97.
33. Leprivier G, Rotblat B, Khan D, Jan E, Sorensen PH. Stress-mediated translational control in cancer cells. *Biochim Biophys Acta*. 2015;1849(7):845–60.
34. Bu Y, Diehl JA. PERK integrates oncogenic signaling and cell survival during cancer development. *J Cell Physiol*. 2016;231(10):2088–96.
35. Holcik M, Sonenberg N. Translational control in stress and apoptosis. *Nat Rev Mol Cell Biol*. 2005;6(4):318–27.
36. Quintin J, Le Peron C, Paliere G, Bizot M, Cunha S, Serandour AA, Avner S, Henry C, Percevault F, Belaud-Rotureau MA, et al. Dynamic estrogen receptor interactomes control estrogen-responsive trefoil factor (TFF) locus cell-specific activities. *Mol Cell Biol*. 2014;34(13):2418–36.
37. Carroll JS, Meyer CA, Song J, Li W, Geistlinger TR, Eeckhoutte J, Brodsky AS, Keeton EK, Fertuck KC, Hall GF, et al. Genome-wide analysis of estrogen receptor binding sites. *Nat Genet*. 2006;38(11):1289–97.
38. Clarke R, Brunner N. Acquired estrogen independence and antiestrogen resistance in breast cancer: estrogen receptor driven phenotypes? *Trends Endocrinol Metab*. 1996;7(8):291–301.
39. Merot Y, Metivier R, Penot G, Manu D, Saligaut C, Gannon F, Pakdel F, Kah O, Flouriot G. The relative contribution exerted by AF-1 and AF-2 transactivation functions in estrogen receptor alpha transcriptional activity depends upon the differentiation stage of the cell. *J Biol Chem*. 2004; 279(25):26184–91.
40. Fox EM, Andrade J, Shupnik MA. Novel actions of estrogen to promote proliferation: integration of cytoplasmic and nuclear pathways. *Steroids*. 2009;74(7):622–7.
41. Le Romancer M, Poulard C, Cohen P, Sentis S, Renoir JM, Corbo L. Cracking the estrogen receptor's posttranslational code in breast tumors. *Endocr Rev*. 2011;32(5):597–622.
42. Yi P, Wang Z, Feng Q, Pintilie GD, Foulds CE, Lanz RB, Ludtke SJ, Schmid MF, Chiu W, O'Malley BW. Structure of a biologically active estrogen receptor-coactivator complex on DNA. *Mol Cell*. 2015;57(6):1047–58.
43. Johansson L, Thomsen JS, Damdimopoulos AE, Spyrou G, Gustafsson JA, Treuter E. The orphan nuclear receptor SHP inhibits agonist-dependent transcriptional activity of estrogen receptors ERalpha and ERbeta. *J Biol Chem*. 1999;274(1):345–53.
44. Hui L, Bakiri L, Mairhorfer A, Schweifer N, Haslinger C, Kenner L, Komnenovic V, Scheuch H, Beug H, Wagner EF. p38alpha suppresses normal and cancer cell proliferation by antagonizing the JNK-c-Jun pathway. *Nat Genet*. 2007; 39(6):741–9.
45. Hansen CA, Bartek J, Jensen S. A functional link between the human cell cycle-regulatory phosphatase Cdc14A and the atypical mitogen-activated kinase Erk3. *Cell Cycle*. 2008;7(3):325–34.
46. Nakamura M, Shimada K, Konishi N. The role of HRK gene in human cancer. *Oncogene*. 2008;27 Suppl 1:S105–113.
47. Accardo A, Trevisiol E, Cerf A, Thibault C, Laurell H, Buscato M, Lenfant F, Amal JF, Fontaine C, Vieu C. Versatile multicharacterization platform involving tailored superhydrophobic SU-8 micropillars for the investigation of breast cancer estrogen receptor isoforms. *J Vac Sci Technol B* 34, 06K201 2016. <http://dx.doi.org/10.1116/1.4962382>.
48. Horigome T, Ogata F, Golding TS, Korach KS. Estradiol-stimulated proteolytic cleavage of the estrogen receptor in mouse uterus. *Endocrinology*. 1988; 123(5):2540–8.
49. Bushell M, Stoneley M, Kong YW, Hamilton TL, Spriggs KA, Dobbyn HC, Qin X, Sarnow P, Willis AE. Polypyrimidine tract binding protein regulates IRES-mediated gene expression during apoptosis. *Mol Cell*. 2006;23(3):401–12.
50. Morfoisse F, Kuchnio A, Frainay C, Gomez-Brouchet A, Delisle MB, Marzi S, Helfer AC, Hantelys F, Pujol F, Guillermet-Guibert J, et al. Hypoxia induces VEGF-C expression in metastatic tumor cells via a HIF-1alpha-independent translation-mediated mechanism. *Cell Rep*. 2014;6(1):155–67.
51. Hanson PJ, Zhang HM, Hemida MG, Ye X, Qiu Y, Yang D. IRES-dependent translational control during virus-induced endoplasmic reticulum stress and apoptosis. *Front Microbiol*. 2012;3:92.
52. Pappin DJI, Hojrup P, Bleasby AJ. Rapid identification of proteins by peptide-mass fingerprinting. *Curr Biol*. 1993;3(6):327–32.

Submit your next manuscript to BioMed Central and we will help you at every step:

- We accept pre-submission inquiries
- Our selector tool helps you to find the most relevant journal
- We provide round the clock customer support
- Convenient online submission
- Thorough peer review
- Inclusion in PubMed and all major indexing services
- Maximum visibility for your research

Submit your manuscript at  
[www.biomedcentral.com/submit](http://www.biomedcentral.com/submit)

